

## Fission and complete-fusion probabilities as a function of angular momentum for $^{170}\text{Yb}$ compound nuclei excited to 107 MeV\*

A. M. Zebelman,<sup>†</sup> L. Kowalski,<sup>‡</sup> J. Miller, K. Beg,<sup>§</sup> Y. Eyal,<sup>¶</sup> G. Jaffe,<sup>||</sup> A. Kandil,<sup>\*\*</sup> and D. Logan  
*Department of Chemistry, Columbia University, New York, New York 10027*

(Received 21 March 1974)

Fission and complete-fusion cross sections are presented for four entrance channels leading to  $^{170}\text{Yb}$  compound nuclei excited to 107 MeV:  $^{11}\text{B} + ^{159}\text{Tb}$ ,  $^{12}\text{C} + ^{158}\text{Gd}$ ,  $^{16}\text{O} + ^{154}\text{Sm}$ , and  $^{20}\text{Ne} + ^{150}\text{Nd}$ . The measured fission cross sections are  $5.9 \pm 0.6$ ,  $16. \pm 2.$ ,  $40. \pm 4.$ , and  $89. \pm 9.$  mb for the  $^{11}\text{B}$ ,  $^{12}\text{C}$ ,  $^{16}\text{O}$ , and  $^{20}\text{Ne}$  entrance channels, respectively. The complete-fusion cross sections for these same entrance channels are  $980 \pm 150$ ,  $1100 \pm 160$ ,  $1260 \pm 190$ , and  $1450 \pm 220$  mb. The data are combined using a technique which yields the dependence of fission probability over three relatively narrow ranges of angular momentum. The results of the analysis just described are compared to a calculation based on the Bohr-Wheeler formalism for fission widths and the Weisskopf formalism for neutron and charged-particle widths. The calculations include the effects of multiple chance fission but assume that second and higher chance fission is nonnegligible only if preceded by neutron emission rather than charged particle emission. Agreement between the experimental results and the theoretical calculations is found for a ratio of level density parameters for the compound nucleus and the saddle point equal to  $1.2 \pm 0.1$ . Fission-fragment angular distributions for the four entrance channels are presented and compared to calculations

NUCLEAR REACTIONS, COMPLETE FUSION, FISSION  $^{159}\text{Tb}(^{11}\text{B}, ^{170}\text{Yb}^*)$ ,  
 $E = 115$  MeV;  $^{158}\text{Gd}(^{12}\text{C}, ^{170}\text{Yb}^*)$ ,  $E = 126$  MeV;  $^{154}\text{Sm}(^{16}\text{O}, ^{170}\text{Yb}^*)$ ,  $E = 137$   
 MeV;  $^{150}\text{Nd}(^{20}\text{Ne}, ^{170}\text{Yb}^*)$ ,  $E = 144$  MeV; measured  $\sigma(\theta)$  for evaporation  
 residues and fission fragments, deduced  $J_{\text{CRIT}}$ ,  $\Gamma_f$ .

### I. INTRODUCTION

The calculation of angular-momentum-independent fission probabilities was first formulated by Bohr and Wheeler within the framework of the statistical model using liquid-drop-model fission barriers.<sup>1</sup> The advent of fast computers allowed the refinement of fission-barrier calculations by Strutinskii, Lyashchenko, and Popov,<sup>2</sup> Cohen and Swiatecki,<sup>3</sup> and Myers and Swiatecki.<sup>4</sup> A number of authors have used the angular-momentum-independent Bohr and Wheeler formalism in the interpretation of their data,<sup>5,6</sup> a notable example being the work of Burnett *et al.*,<sup>7</sup> which outlined a general approach to the calculation of fission probabilities for systems with zero angular momentum.

As energetic particle beams, especially of heavy ions, became available to experimenters<sup>8-19</sup> the effects of angular momentum on the fission process had to be taken into account. Studies by Pik-Pichak,<sup>20,21</sup> Hiskes,<sup>22</sup> and Plasil<sup>23</sup> were concerned with the effect of angular momentum on the fission barrier. Recently, Gadioli *et al.*<sup>24</sup> have modified the approach of Burnett *et al.*<sup>7</sup> to include the effects of angular momentum in the calculation of fission probabilities.

This present work concerns itself with the ex-

perimental determination of the effects of angular momentum on the fission probability of a particular compound nucleus and with a comparison of the results with current theoretical predictions. In addition, fission-fragment angular distributions are presented and the role of angular momentum in their determination discussed. This latter aspect of the present study is a continuation of work previously reported.<sup>19</sup>

The compound nucleus chosen for study was  $^{170}\text{Yb}$ . A relatively light-mass system was selected in order that the angular-momentum dependence of the fission probability not be masked by a fission probability close to unity due to a low fission barrier combined with the high excitation energies produced in heavy-ion reactions. Production of  $^{170}\text{Yb}$  via a heavy-ion entrance channel is indicated in order to produce compound nuclei with significant amounts of angular momentum. The particular choice of  $^{170}\text{Yb}$  for study was dictated by the heavy-ion beams available at the Yale University heavy-ion accelerator and by the isotopically enriched targets available from Oak Ridge National Laboratory.

Bombardments with heavy ions produce compound nuclei with a broad distribution of angular momenta. The large range of this distribution makes the average angular momentum a quantity

of uncertain value in data analysis. However, a method of analysis, to be outlined in Sec. III, has been previously developed which allows the calculation of partial cross sections for events arising from compound nuclei characterized by a relatively narrow range of angular momenta.<sup>17, 25</sup> Characterizing these relatively narrow angular-momentum distributions by their average, now more sharply defined, in principle allows the more accurate determination of the angular-momentum dependence of the phenomena (in this case fissionability) under study. The method of analysis requires data obtained from a number of different entrance channels forming the same compound nucleus at the same excitation energy, but which differ only in their angular-momentum distributions. The calculation of fission probability and its dependence on angular momentum requires the measurement of both the fission and complete-fusion cross sections for the entrance channels concerned.

The reactions which formed the entrance channels of <sup>170</sup>Yb in this work are: <sup>11</sup>B + <sup>159</sup>Tb, <sup>12</sup>C + <sup>158</sup>Gd, <sup>16</sup>O + <sup>154</sup>Sm, and <sup>20</sup>Ne + <sup>150</sup>Nd. The beam energies were chosen so as to produce an excitation energy of 107 MeV.

## II. EXPERIMENTAL

The heavy-ion bombardments were carried out at the Yale University heavy-ion accelerator. The beam energies necessary to produce the desired excitation energies were calculated with the nuclidic mass tables given in Ref. 26 and are listed in Table I. Beams of energy less than 10.5 MeV/nucleon were obtained by the insertion of the appropriate degrading foils upstream of the accelerator's double-focusing system consisting of two quadrupoles and two 45° bending magnets. This system exhibits an energy resolution of about 1%.

The physical characteristics of the scattering chamber used in this work are fully described in Ref. 25. The chamber's height and lateral position were adjusted so that the centers of the upstream chamber port, and the target mount intersected

the beam axis. The beam axis was located with a transit.

The heavy-ion beams were collected in a magnetically protected Faraday cup and the current integrated with an Elcor integrator.

### A. Fission cross sections

Self-supporting and isotopically enriched targets of <sup>158</sup>Gd, <sup>154</sup>Sm, and <sup>150</sup>Nd were obtained from Oak Ridge National Laboratory. Their thicknesses were determined gravimetrically. The <sup>159</sup>Tb target, an isotope whose natural abundance is 100%, was prepared by evaporation of the metal<sup>27</sup> onto a carbon film<sup>28</sup> of about 40 μg/cm<sup>2</sup>. Its thickness and the isotopic enrichments of the other targets are included in Table I.

Solid-state detectors were used in some of the fission cross-section measurements. Two detector telescopes were available. One, located 5.10 cm from the target, was used at angles where its large solid angle did not result in prohibitively high counting rates. The other telescope was located 22.2 cm from the target and was used at angles where use of the former telescope was contraindicated. An aluminum block was placed at the side of the target to prevent beams scattered from the antiscattering collimator from entering telescopes placed between 0 and 30°. Aluminum collimators 0.158 cm thick and of various known dimensions were placed in the detector telescopes and served both to define their solid angles and to prevent particles from hitting the edges of the detectors.

The detector stack used in the telescopes consisted of a 9-μm detector upstream of a 3-mm detector. A very thin upstream detector was chosen because scattered beam and other particles whose masses are small compared to those of fission fragments deposit little energy in such a detector. Fission fragments, on the other hand, deposit all or most of their energy in a 9-μm detector. The 3-mm detector was used to monitor the scattered beam in order that beam intensities could be adjusted so as not to give prohibitively high counting rates.

TABLE I. General details of the fission and complete-fusion experiments. The column headings are self-explanatory.

Entrance channel	Lab energy	Excitation energy	Fission targets		CF targets	
			Thick. (mg/cm <sup>2</sup> )	Abd. (%)	Thick. (mg/cm <sup>2</sup> )	Abd. (%)
<sup>11</sup> B + <sup>159</sup> Tb	115	107	1.58	100	0.162	100
<sup>12</sup> C + <sup>158</sup> Gd	126	107	1.00	98	1.00	98
<sup>16</sup> O + <sup>154</sup> Sm	137	107	0.87	99	0.87	99
<sup>20</sup> Ne + <sup>150</sup> Nd	144	107	1.01	95	0.216	natural

Muscovite-mica track detectors were also used in the measurement of the fission cross sections for the  $^{11}\text{B}$ ,  $^{12}\text{C}$ ,  $^{16}\text{O}$ , and  $^{20}\text{Ne}$  entrance channels. The use of mica track detectors allowed the use of the largest available beam intensities and yielded more accurate angular-distribution data than did the experiments involving solid-state detectors.

The mica detectors were die cut to  $3.8 \times 3.18$  cm and were about  $20 \text{ mg/cm}^2$  in thickness.<sup>29</sup> Each piece of mica was etched in 48% hydrofluoric acid for three hours prior to use in order to enlarge the tracks already in the mica to large diamond-shaped tracks easily distinguishable from properly developed fission tracks. The mica detectors were mounted such that the beam line fell 1.3 cm from the tops of the pieces of mica. Following

exposure, the pieces of mica were etched in 48% hydrofluoric acid for 30 minutes at room temperature. Each piece of mica was then scanned at  $1185 \times$  and a record kept of the number of fission events in a field of view of known area and angle with respect to the beam, and of known distance from the target. The Faraday cup was used for the determination of the beam current in those runs in which mica detectors were placed at  $10^\circ$  intervals between  $10$  and  $170^\circ$ . For angles less than  $10^\circ$ , the beam current was monitored by the elastic scattering into a solid-state monitor detector.

#### B. Complete-fusion cross sections

The targets for the determination of the complete-fusion cross sections for the  $^{12}\text{C}$  and  $^{16}\text{O}$

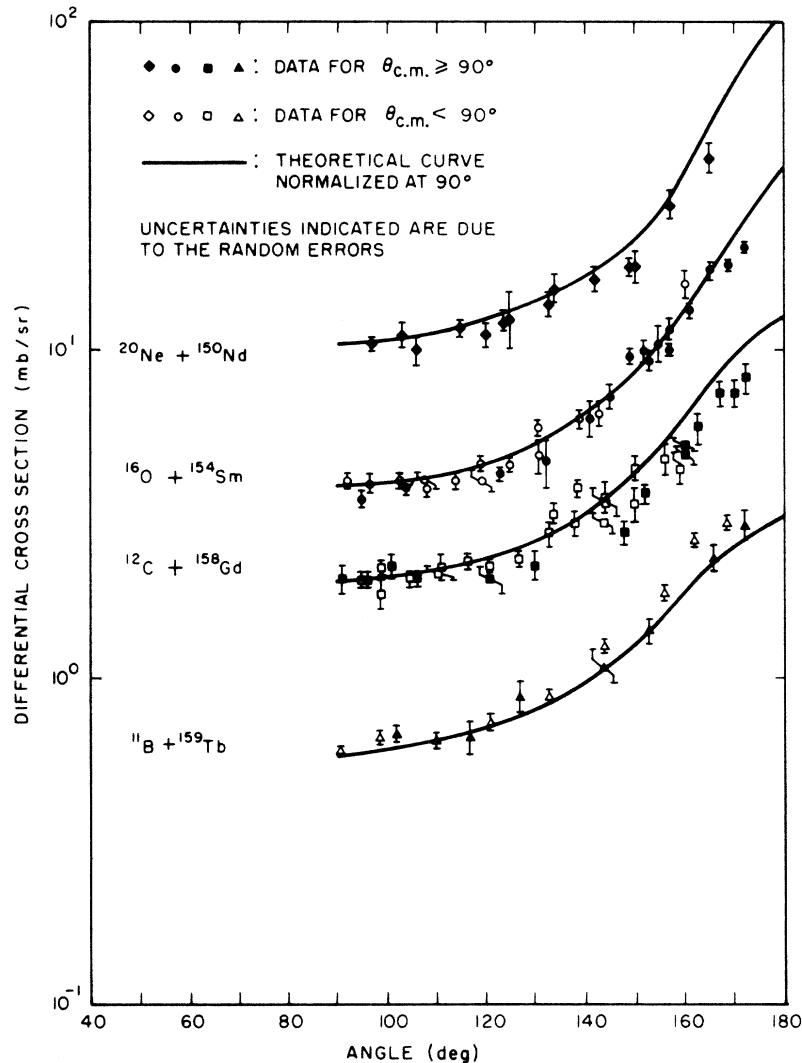


FIG. 1. Center-of-mass fission-fragment angular distributions for the four  $^{170}\text{Yb}$  entrance channels studied in this work. The curves are theoretical with normalization at  $90^\circ$ .

TABLE II. Cross sections for the fission and complete-fusion experiments including the contribution from fission.

Entrance channel	Excitation energy (MeV)	Total fission cross section (mb)	Total complete-fusion cross section (mb)
$^{11}\text{B} + ^{159}\text{Tb}$	107	$5.9 \pm 0.6$	$980 \pm 150$
$^{12}\text{C} + ^{158}\text{Gd}$	107	$16 \pm 2$	$1100 \pm 160$
$^{16}\text{O} + ^{154}\text{Sm}$	107	$40 \pm 4$	$1260 \pm 200$
$^{20}\text{Ne} + ^{150}\text{Nd}$	107	$89 \pm 9$	$1450 \pm 220$

entrance channels were the same as those used in the fission cross-section measurements. Targets for the complete-fusion cross-section measurements for the  $^{11}\text{B}$  and  $^{20}\text{Ne}$  entrance channels were prepared from metal of naturally occurring isotopic abundance. The metals were obtained in 99.9% purity from A. D. MacKay, Incorporated.<sup>27</sup> The target materials were vacuum evaporated onto carbon films about  $40 \mu\text{g}/\text{cm}^2$  thick. The fact that the neodymium targets for the complete-fusion work consisted of the metal in its natural isotopic abundance was not expected to affect the experimental results as it is the atomic charges of the target and projectile which are expected to be of paramount importance in these reactions. The thicknesses of these targets were determined by measuring the elastic scattering cross sections and are included in Table I.

Following the work of Kowalski, Jodogne, and Miller,<sup>30</sup> muscovite-mica track detectors were used in the complete-fusion cross-section measurements. The mica detectors were prepared as described in the previous section, except that they were cleaved prior to their prebombardment etching so as to have a surface as free of defects as possible. The cleaved mica had a thickness of about  $10 \text{ mg}/\text{cm}^2$ . The true  $0^\circ$  line was determined by comparing cross sections determined by a mica detector placed at  $-10^\circ$  with those in a similar detector placed at  $+10^\circ$ . Scanning of the mica was carried out as it was for the fission experiments.

### III. RESULTS

#### A. Fission cross sections

The fission cross section for 126 MeV  $^{12}\text{C}$  on  $^{197}\text{Au}$  was measured as a check on the efficiency of the solid-state detector system that was used to collect some of the fission-cross-section data. Integration of the angular distribution yields a total fission cross section of  $1.3 \pm 0.1 \text{ b}$ , compared to a previously reported value of  $1.35 \pm 0.1 \text{ b}$ .<sup>31</sup>

The results of fission experiments using mica

detectors agreed quite well with the measurements carried out with the solid-state detectors; this then verified both that the fission fragments were registering in the mica with 100% efficiency, and that the identification of fission tracks was being made correctly.

The center-of-mass differential fission cross sections that were measured are shown in Fig. 1. These cross sections were calculated from the measured laboratory cross sections in the manner described by Sikkeland, Lansky, and Gordon<sup>32</sup> by assuming that all the fragments had a single mass, 85 amu, and a single center-of-mass kinetic energy of 57 MeV, as suggested by the results of Viola and Sikkeland.<sup>33</sup> As pointed out by Britt and Quinton,<sup>11</sup> because of the symmetric nature of the fission distribution a negligible error in the transformation results from substituting the average values instead of the distributions of mass and energy of the fission fragments.

The fission cross sections obtained by integrating the angular distribution of Fig. 1 are given in Table II. The errors quoted include the uncertainty in extrapolating the angular distributions to  $0^\circ$ .

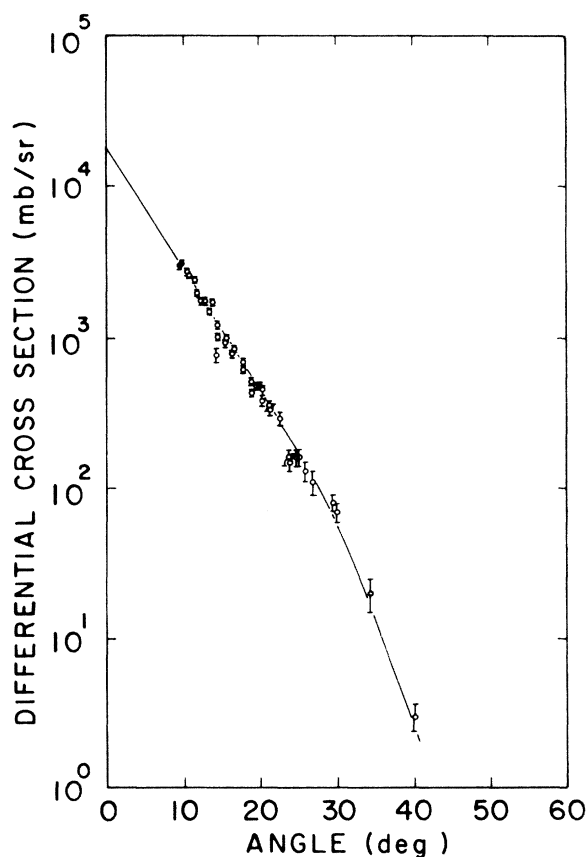


FIG. 2. The complete-fusion angular distribution for 115 MeV  $^{11}\text{B} + ^{159}\text{Tb}$ .

### B. Complete-fusion cross sections

There is the concern that there might be less than 100% registration efficiency in mica for the complete-fusion recoils produced in the present experiments because of the low kinetic energy of these products. In order to check this point, data were collected in separate experiments with the target perpendicular to the beam and at  $45^\circ$  with respect to the beam. It was expected that if indeed one was at an energy threshold for 100% registration, there would be a large discrepancy in the cross sections measured; no such discrepancy was found. Further, measurements of the complete-fusion cross section in the  $^{11}\text{B}$ - $^{159}\text{Tb}$  system with counter-telescope detection is in good agreement with that determined by the mica technique.<sup>34</sup>

In addition to the problem of the registration threshold, one must consider the uncertainties introduced in identifying complete-fusion tracks. All events which had the appearance of a track and which were not fission tracks were counted as complete-fusion events. As the complete-fusion tracks were quite small, track identification was difficult at times. It is the error inherent in the

scanning that makes the major contribution to the uncertainty in the complete-fusion cross sections.

The complete-fusion angular distributions are shown in Figs. 2-5. Integration of these angular distributions yields the cross sections that are given in Table II.

There are a few features of the complete-fusion angular distributions that merit comments: The first feature is that of the angular spread of the distributions. The data from the  $^{12}\text{C}$  and  $^{16}\text{O}$  entrance channels exhibit much broader angular distributions than do the data from the  $^{11}\text{B}$  and  $^{20}\text{Ne}$  entrance channels. This is a direct consequence of the much thicker targets that were used in the collection of the data in the former entrance channels. Referring to Fig. 5, the second feature of interest is the anomalous "bump" at about  $15^\circ$  in the  $^{20}\text{Ne}$  complete-fusion angular distribution. The data shown are the results of three separate experiments, two of which yielded data in the region of concern. A rough estimate of the cross section for the reactions that give rise to the bump may be made by assuming that all of the cross section for angles greater than  $15^\circ$  contribute. Under this assumption the cross section is about 90 mb.

It is conceivable that the "bump" might arise from any or all of three extraneous sources:

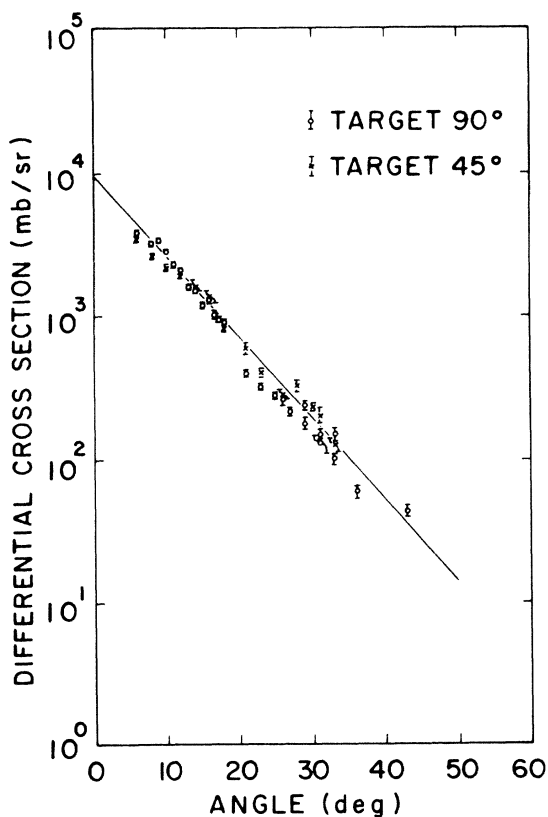


FIG. 3. The complete-fusion angular distribution for 126 MeV  $^{12}\text{C} + ^{158}\text{Gd}$ .

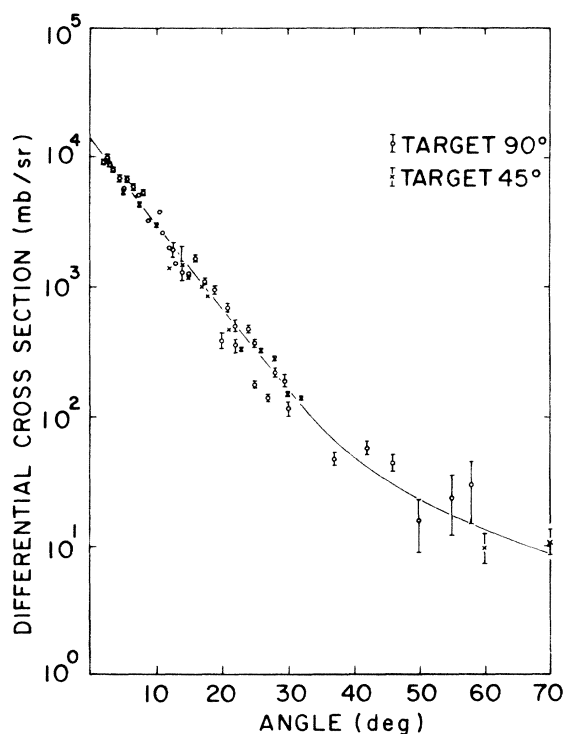


FIG. 4. The complete-fusion angular distribution for 137 MeV  $^{16}\text{O} + ^{154}\text{Sm}$ .

- (1) target nuclei recoiling from elastic scattering of the projectile;
- (2) transfer reactions in which the projectile picks up nucleons and then has enough mass and energy to produce a track in mica;
- (3) heavy recoil products arising from transfer reactions in which the target nucleus picks up nucleons.

If the "bump" is attributed to elastically scattered target nuclei, then kinematics requires the  $^{20}\text{Ne}$  projectiles to be scattered to laboratory angles of  $145^\circ$  and larger. An optical model calculation shows the cross section for such events to be of the order of 10's of microbarns, and therefore much too small to account for the "bump."

A review of the literature would seem to eliminate projectile pick-up reactions as the source of the "bump." Experiments have shown that cross sections for pick-up reactions of the type that would be required are quite small.<sup>35-39</sup>

The registration of heavy recoil products arising from multinucleon transfer reactions may explain the "bump" in the angular distribution. Kinematic calculations in which it is assumed that the light residual products will have the same energy per

nucleon as the incident  $^{20}\text{Ne}$ , show that reactions which result in the transfer of 10 nucleons or more will give rise to heavy recoils all of which will register in mica. Only a diminishing fraction of the reactions corresponding to less than a 10-nucleon transfer will register. For example, the transfer of  $^8\text{Be}$  to the target nucleus, which results in  $^{12}\text{C}$  in the exit channel, will give rise to a heavy residual nucleus with enough energy to register in the mica only when the  $^{12}\text{C}$  appears at angles greater than  $30^\circ$  in the laboratory. An estimate of cross sections for such multinucleon transfer reactions was made by bombarding the  $^{158}\text{Gd}$  target with 144 MeV  $^{20}\text{Ne}$  since unfortunately, at the time of this experiment a Nd target was no longer available. However, as noted by Croft, Alexander, and Street<sup>40</sup> the transfer cross sections are not expected to be very sensitive to a small change in the atomic number of the target. The sum of the cross sections for transfer reactions which result in the formation of Li, Be, and B products was found to be  $50 \pm 10$  mb. The cross section for producing C in the exit channel at laboratory angles greater than  $30^\circ$  is  $42 \pm 4$  mb out of a total cross section over all angles of  $80 \pm 8$  mb. Thus it is expected that multinucleon transfer reactions will result in the  $^{20}\text{Ne}$  complete fusion cross section being about 100 mb too large, in good agreement with the magnitude of the cross section attributed to the "bump." The value of the  $^{20}\text{Ne}$  cross section listed in Table II reflects this correction.

A question arises now as to the effect of multinucleon transfer reactions in the other entrance channels studied. Kinematic calculations show that as the mass of the incident projectile decreases from  $^{20}\text{Ne}$  to  $^{11}\text{B}$  there is a corresponding increase in the minimum angle at which a product that registers in mica would appear. There is also a corresponding increase in the laboratory angle of its light partner. Differential cross sections of such light products are well known to decrease sharply with increasing angle.<sup>37-39, 41, 42</sup> Thus it is expected that the registration of direct reaction events will make an ever-decreasing contribution to the measured complete fusion cross section as one goes from  $^{20}\text{Ne}$  to  $^{11}\text{B}$ .

#### IV. DISCUSSION

In the following paragraphs there is discussed the treatment of the experimental data in a manner that yields the angular-momentum dependence of fissionability. The results are then compared to theoretical calculations of this quantity. An analysis is also made of the fission-fragment angular distributions for the  $^{11}\text{B}$ ,  $^{12}\text{C}$ ,  $^{16}\text{O}$ , and  $^{20}\text{Ne}$  entrance channels.

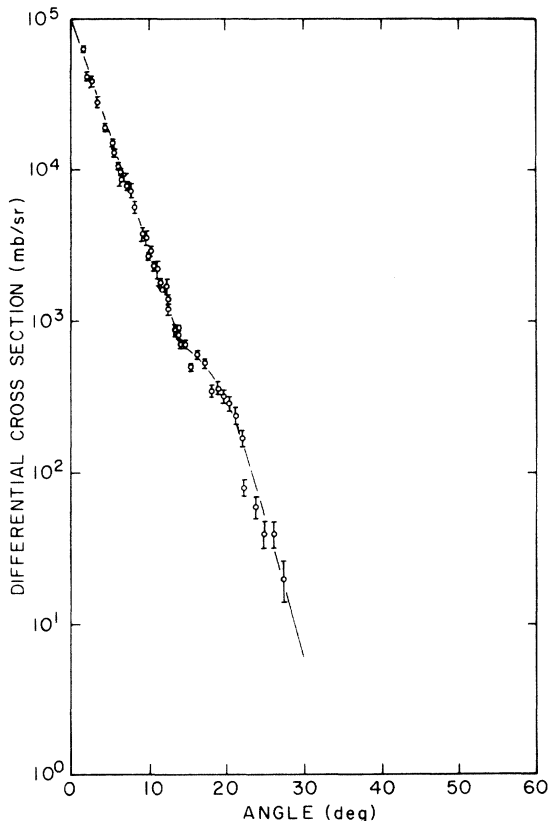


FIG. 5. The complete-fusion angular distribution for 144 MeV  $^{20}\text{Ne} + ^{160}\text{Nd}$ .

### A. Fissionability calculations from experimental data

The probability that a compound nucleus formed via an entrance channel  $x$  with a given initial excitation energy will undergo fission at some point in its deexcitation is just:

$$\sigma_f(x)/\sigma_{cf}(x), \quad (1)$$

where  $\sigma_f$  is the cross section for compound-nuclear fission and  $\sigma_{cf}$  is the complete-fusion cross section.

In order to extract the angular-momentum dependence of fission probability from the experimental cross sections one may exploit the Bohr independence hypothesis. According to the Bohr hypothesis, the compound-nucleus fission cross section for a particular entrance channel,  $x$ , may be written:

$$\sigma_f(x) = \sum_{J=0}^{\infty} \sigma_{cf}(x|J)W_f(J), \quad (2)$$

where  $\sigma_{cf}(x|J)$  is the cross section for the formation of the compound nucleus characterized by a given excitation energy and by a given angular momentum  $J$  in the entrance channel  $x$ ;  $W_f(J)$  is the probability that the compound nucleus with the given angular momentum and excitation energy will fission. The independence hypothesis demands that  $W_f(J)$  be purely a property of the compound nucleus and thus is independent of its mode of formation. The partial complete-fusion cross section is given by:

$$\sigma_{cf}(x|J) = \pi\lambda_x^2 \frac{(2J+1)}{(2s+1)(2j+1)} \sum_{S=|j-s|}^{j+s} \sum_{l=|J-S|}^{J+S} T_l'(x), \quad (3)$$

where  $s$  and  $j$  are the projectile and target spins, respectively;  $S$  is the channel spin,  $J$  is the total angular momentum, and  $T_l'(x)$  is the transmission coefficient for compound-nucleus formation in entrance channel  $x$ .

When  $s=j=0$ , as is the case for the  $^{12}\text{C}$ ,  $^{16}\text{O}$ ,  $^{20}\text{Ne}$  entrance channels, Eq. (3) reduces to:

$$\sigma_{cf}(x|J) = \pi\lambda_x^2 (2J+1) T_{l=J}'(x). \quad (4)$$

One also obtains Eq. (4) for the  $^{11}\text{B}$  entrance channel, where  $s=j=\frac{3}{2}$ , if  $J > 3\hbar$  and  $T_l'(x)$  is independent of  $l$  over the  $J$  region of interest. The deviation of Eq. (4) from Eq. (3) for  $J < 3\hbar$  will have a negligible effect on the results to come. The independence of  $T_l'$  and  $l$  over the  $J$  region of interest holds true under the sharp-cutoff approximation for  $\sigma_{cf}(x|J)$  since, as we shall see later,  $T_l = 1$  over that region. Hereafter  $T_{l=J}'(x)$  will be written as  $T_J'(x)$ .

Upon substituting Eq. (4) in Eq. (2) we find:

$$\sigma_f(x) = \pi\lambda_x^2 \sum_{J=0}^{\infty} (2J+1) T_J'(x) W_f(J) \quad (5)$$

and  $\sigma_{cf}(x)$  in Eq. (1) may be written:

$$\sigma_{cf}(x) = \pi\lambda_x^2 \sum_{J=0}^{\infty} (2J+1) T_J'(x). \quad (6)$$

If the ratio of Eq. (5) to Eq. (6) is taken, in accord with the prescription of Eq. (1),

$$\begin{aligned} \frac{\sigma_f(x)}{\sigma_{cf}(x)} &= \frac{\sum_{J=0}^{\infty} (2J+1) T_J'(x) W_f(J)}{\sum_{J=0}^{\infty} (2J+1) T_J'(x)} \\ &\equiv \langle W_f(J) \rangle_x. \end{aligned} \quad (7)$$

The expected result is obtained that the ratio of the fission to complete-fusion cross section is just  $W_f(J)$  averaged over the entire spin distribution of entrance channel  $x$ .

As shown in Refs. 43–45 when data are available from a number of entrance channels that lead to compound nuclei of the same  $Z, A$ , and excitation energy, use of the Bohr independence hypothesis allows the isolation and study of the behavior of compound nuclei having a range of angular momenta which is much narrower than the spin distribution in any one of the particular entrance channels. To see this, consider equations analogous to Eqs. (5) and (6) for another corresponding entrance channel  $y$ :

$$\sigma_f(y) = \pi\lambda_y^2 \sum_{J=0}^{\infty} (2J+1) T_J'(y) W_f(J) \quad (8)$$

and

$$\sigma_{cf}(y) = \pi\lambda_y^2 \sum_{J=0}^{\infty} (2J+1) T_J'(y). \quad (9)$$

If Eqs. (5), (6), (8), and (9) are divided by their respective values of  $\pi\lambda^2$  (from this point on, any cross section  $\sigma$  divided by  $\pi\lambda^2$  for the corresponding entrance channel will be denoted by  $\sigma'$ :  $\sigma' = \sigma/\pi\lambda^2$ ) and differences taken between Eqs. (5) and (8) as well as Eqs. (6) and (9), there results:

$$\sigma_f'(x) - \sigma_f'(y) = \sum_{J=0}^{\infty} (2J+1) W_f(J) [T_J'(x) - T_J'(y)], \quad (10)$$

$$\sigma_{cf}'(x) - \sigma_{cf}'(y) = \sum_{J=0}^{\infty} (2J+1) [T_J'(x) - T_J'(y)]. \quad (11)$$

There are two central points that are to be noted: (i) It is the independence hypothesis that allows the factoring of  $W_f(J)$  in Eq. (10), and

(ii) The quantities on the left-hand sides of Eqs. (10) and (11) represent cross sections for compound nuclei within the relatively narrow range of  $J$  for which  $T'_f(x) - T'_f(y) \neq 0$ .

If now the ratio of Eq. (10) to Eq. (11) is taken:

$$\frac{\sigma'_f(x) - \sigma'_f(y)}{\sigma'_{cf}(x) - \sigma'_{cf}(y)} = \frac{\sum_{J=0} (2J+1)W_f(J)[T'_f(x) - T'_f(y)]}{\sum_{J=0} (2J+1)[T'_f(x) - T'_f(y)]} = \langle W_f(J) \rangle_{x-y}. \quad (12)$$

The result is the average fission probability over the region of  $J$  for which  $T'_f(x) - T'_f(y) \neq 0$ .

In the present experiment it is clearly possible to identify three such regions  $^{12}\text{C}$ - $^{11}\text{B}$ ,  $^{16}\text{O}$ - $^{12}\text{C}$ , and  $^{20}\text{Ne}$ - $^{16}\text{O}$ , which we shall denote as regions I, II, and III, respectively. Thus, for example,

$$\frac{\sigma'_f(\text{II})}{\sigma'_{cf}(\text{II})} = \frac{\sigma'_f(^{16}\text{O}) - \sigma'_f(^{12}\text{C})}{\sigma'_{cf}(^{16}\text{O}) - \sigma'_{cf}(^{12}\text{C})} \equiv \langle W_f(J) \rangle_{\text{II}}. \quad (13)$$

The values of  $\langle W_f(J) \rangle_x$  and  $\langle W_f(J) \rangle_{\text{I-III}}$  that are obtained in this manner are listed in the fourth column of Table III. These average probabilities come directly from the experimental data without the interposition of any model-dependent theoretical estimates. The angular-momentum distribution over which they are the average, however,

TABLE III. Comparison of experimental and theoretical values of fission probability.

Region	$J_{\text{CRIT}}$ (h)	$J$ range (h)	$[W_f(J)]_{\text{exp.}}$	$[W_f(J)]_{\text{theor.}}$
$^{11}\text{B}$	$40 \pm 3$	0-40	$0.006 \pm 0.001$	$0.006^{+0.001}_{-0.001}$
$^{12}\text{C}$	$46 \pm 4$	0-46	$0.015 \pm 0.003$	$0.011^{+0.003}_{-0.004}$
$^{16}\text{O}$	$58 \pm 4$	0-58	$0.032 \pm 0.006$	$0.038^{+0.012}_{-0.018}$
$^{20}\text{Ne}$	$70 \pm 6$	0-70	$0.060 \pm 0.01$	$0.14^{+0.16}_{-0.08}$
I		41-46	$0.04 \pm 0.03$	$0.017^{+0.003}_{-0.001}$
II		47-58	$0.06 \pm 0.03$	$0.066^{+0.001}_{-0.02}$
III		59-70	$0.12 \pm 0.07$	$0.34^{+0.3}_{-0.07}$

requires an estimate of the  $T'_f$  in each entrance channel. This estimate is carried out in the following section.

#### B. Complete-fusion transmission coefficients

The transmission coefficients  $T_f(X)$ , as distinct from the  $T'_f(x)$ , may be calculated within the framework of the optical model. This was done using the optical model code ABACUS-2<sup>46</sup> with parameters from Auerbach and Porter.<sup>47</sup> The resulting transmission coefficients and the partial

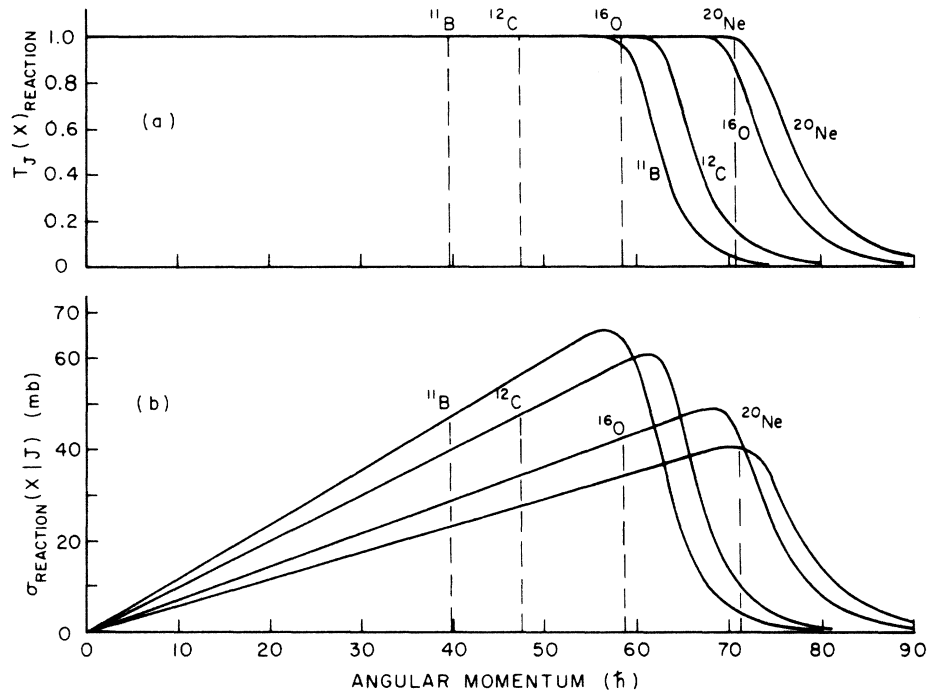


FIG. 6. Optical model: (a) transmission coefficients, and (b) partial reaction cross sections for the four entrance channels of interest. The dotted lines are the sharp-cutoff approximation from the measured complete-fusion cross sections.



cross sections for the  $^{11}\text{B}$ ,  $^{12}\text{C}$ ,  $^{16}\text{O}$ , and  $^{20}\text{Ne}$  entrance channels are shown in Figs. 6(a) and 6(b), respectively. The fact that these are transmission coefficients and partial cross sections for the *total* reaction cross sections means that  $T_j'(x)$  and  $\sigma_{CF}(x|J)$  are but a subset of them. Thus, one must appeal to another model to separate the transmission coefficients and the partial cross sections for complete fusion from the larger set characterizing the total reaction cross sections.

The model generally chosen to accomplish this is the sharp-cutoff model. According to this model, the set of partial cross sections for complete fusion in a particular entrance channel may be found by summing from  $J=0$  the partial cross sections calculated with the optical model until the sum of the partial cross sections most closely equals the experimentally measured complete-fusion cross section. The largest value of  $J$  which contributes to the complete-fusion cross sections is termed  $J_{\text{CRIT}}$ . All the transmission coefficients and partial cross sections corresponding to  $J$  values in excess of  $J_{\text{CRIT}}$  are taken to refer to transfer reactions and inelastic scattering. In general, there is a different  $J_{\text{CRIT}}$  for each entrance channel. The values of  $J_{\text{CRIT}}$  estimated in this manner for the entrance channels investigated here are included in Table III and define the angular-momentum regions over which the fission probabilities are averaged.

The justification of the sharp-cutoff approximation arises from studies of direct reactions which show that these reactions are evidently nuclear-surface reactions.<sup>48</sup> In other words, direct reactions are characterized by relatively large impact parameters and concomitantly large values of angular momentum. A sharp cutoff is made at  $J_{\text{CRIT}}$  since the paucity of data concerning the angular momentum dependence of direct reactions does not at this time justify a more refined approximation. However, an attempt was made to determine the effect of not demanding a sharp cutoff in  $\sigma_{CF}(x|J)$  at  $J_{\text{CRIT}}$ . Instead,  $\sigma_{CF}(x|J)$  was taken to be the same as  $\sigma_R(x|J)$  (the partial reaction cross section for entrance channel  $x$ ) up to some angular momentum  $J'$  and then required to vanish linearly at  $J'_{\text{CRIT}}$ . The sum over  $J$  of  $\sigma_{CF}(x|J)$  was, of course, still required to equal the experimental values of  $\sigma_{CF}(x)$ . The calculations were parametrized in terms of  $\Delta$  defined as:

$$\Delta = J'_{\text{CRIT}} - J'.$$

Clearly, this alternate model reduces to the sharp cutoff model when  $\Delta = 0$ . An illustration of this model is shown in Fig. 7. Variations of  $\Delta$  up to  $10\hbar$  are found to yield fission probabilities, calculated in a fashion to be described in the fol-

lowing section, that do not differ markedly from those calculated with the sharp-cutoff approximation.

Having discussed the estimation of  $T_j'(x)$ , we now turn to a comparison between calculated and measured fission probabilities.

### C. Fission probability

At high excitation energies fission may occur at any one of several points in the decay of the initial compound nucleus. In general, then, one must deal with the possibility of fission occurring from parent nuclei having a spectrum of excitation energies and angular momenta. In order to make the fission-probability calculations tractable, a number of assumptions are made:

- (1) Competition between fission and neutron, proton, or  $\alpha$  particle emission is allowed at each step. Competition with  $\gamma$ -ray emission is ignored.
- (2) Residual nuclei which arise as a result of proton or  $\alpha$ -particle emission are assumed to have a negligible chance of fissioning.
- (3) Evaporated neutrons are assumed to carry off no angular momentum; i.e., the angular-momentum distribution which characterized the initial compound nuclei also characterizes the nuclei resulting from neutron evaporation.

In accord with the above assumptions, the fission probability depends on the quantities  $\Gamma_f(J)$ ,  $\Gamma_n(J)$ ,  $\Gamma_\alpha(J)$ , and  $\Gamma_p(J)$ , which are the angular-momentum- and excitation-energy-dependent widths for fission, neutron,  $\alpha$ , and proton emission, respectively, along the decay chain. For ease of later reference, let us define

$$\Gamma_T(J) = \Gamma_n(J) + \Gamma_p(J) + \Gamma_\alpha(J). \quad (14)$$

The calculation of  $W_f(J)$  proceeds as follows: (1)  $\Gamma_f(J)$  and  $\Gamma_T(J)$  are calculated for the initial compound nucleus  $^{170}\text{Yb}$  excited to 107 MeV; (2) the spectrum of residual excitation energies for  $^{169}\text{Yb}$

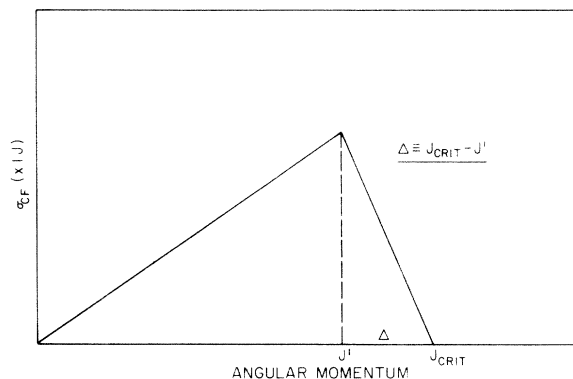


FIG. 7. Illustration of the alternate model to the sharp-cutoff model.

is determined from an evaporation calculation, and this spectrum of energies is then used in the calculation  $\Gamma_f(J)$  and  $\Gamma_T(J)$  for  $^{169}\text{Yb}$ . As noted above, the spin distribution which characterized  $^{170}\text{Yb}$  is assumed to characterize the residual nucleus also; (3) steps analogous to (2) are re-

peated until the fission width becomes negligible compared to  $\Gamma_T(J)$ . For this system, this occurs after the emission of two or three neutrons. The quantity  $\Gamma_T(J)$  was calculated using an angular-momentum-dependent evaporation code called EVAMCO.<sup>49</sup> The code calculates the angular-mo-

mentum-dependent particle emission width according to

$$\Gamma_\nu(J) = \frac{1}{2\pi\rho(E^0, J)} \int_0^{E_{\max}} dE \sum_{J_f} \rho(E_{\max} - E, J_f) \sum_{s=|J_f-s_\nu|}^{J_f+s_\nu} \sum_{l=|J-s|}^{J+s} T_l(\nu), \quad (15)$$

where the emitted particle  $\nu$  is characterized by channel energy  $E$  and spin  $s_\nu$ , and  $J_f$  is the angular momentum of the residual nucleus.  $E_{\max}$  is given by

$$E_{\max} = E^0 - B_\nu - \Delta_\nu, \quad (16)$$

where  $B_\nu$  is the binding energy of particles in the compound nucleus and  $\Delta_\nu$  is the usual parameter to correct for odd-even effects. The level density  $\rho(E, J)$  was taken to be

$$\rho(E, J) = \frac{(2J+1)\omega(E)}{\pi^{1/2}(2\sigma^2)^{3/2}} \exp[-J(J+1)/2\sigma^2], \quad (17)$$

where the so-called spin cutoff parameter  $\sigma$  is

$$\sigma^2 = \mathcal{I}t/\hbar^2. \quad (18)$$

$\mathcal{I}$  is the effective nuclear moment of inertia and  $t$  is the nuclear temperature of the compound nucleus. The nuclear temperature is related to the excitation energy  $E$  by

$$E = at^2 - t, \quad (19)$$

where  $a$  is the level density parameter of the compound nucleus. The state density  $\omega(E)$  in Eq. (17) is

$$\omega(E) = [(E - \Delta) + t]^{-5/4} \exp\{2[a(E - \Delta)]^{1/2}\}. \quad (20)$$

A discussion of the values chosen for the parameters in Eqs. (16)–(20) is postponed until after the calculations of the fission width  $\Gamma_f(J)$  is discussed.

The calculation of the fission width is based on the formalism developed by Bohr and Wheeler.<sup>1</sup> Within that formalism, the average fission width for levels of a particular spin and parity is given as

$$\Gamma_f(J, \pi) = [D(E, J, \pi)/2\pi] N_f(J, \pi), \quad (21)$$

where  $N_f(J, \pi)$  is the effective number of open channels in the transition state nucleus and  $D(E, J\pi)$  is the average level spacing in the compound nucleus at excitation energy  $E$  for levels of spin  $J$  and parity  $\pi$ .

In a more complete analysis of the number of open channels at the transition state the effects

of fission-barrier penetration must be included. Hill and Wheeler derive the following penetrability formula for an inverted harmonic oscillator potential barrier<sup>50</sup>:

$$P(T) = \frac{1}{[1 + \exp(-2T/\hbar\omega)]}, \quad (22)$$

where  $\omega$  is the vibrational frequency of the harmonic oscillator having a potential energy function given by the negative of the potential energy function describing the barrier. The maximum kinetic energy in the fission degree of freedom  $T_m$  is given by

$$T_m = E^0 - B_f, \quad (23)$$

where  $B_f$  is the barrier to fission.

The characteristic quantum energy  $\hbar\omega$  is fixed by the curvature of the top of the barrier and the reduced mass of the system.

Under the assumption that the level spectrum of the saddle point for both parities at any excitation energy  $U$  may be represented by a level density  $\rho^*(U, J)$ , the fission width for a particular value of  $J$ , including the effects of barrier penetrability, is

$$\Gamma_f(J) = \frac{1}{2\pi\rho(E^0, J)} \times \int_0^{E^0} d\epsilon \frac{\rho^*(\epsilon, J)}{1 + \exp[-2\pi(E^0 - B_f - \epsilon)/\hbar\omega]}, \quad (24)$$

where  $\epsilon$  is the energy in the nonfission degrees of freedom, and is related to  $E^0$ ,  $B_f$ , and  $T$  by:

$$\epsilon = E^0 - B_f - T. \quad (25)$$

The form of the level densities indicated in Eq. (24) is the same as used in the  $\Gamma_T$  calculations given in Eq. (17).

With the expressions for  $\Gamma_f(J)$  and  $\Gamma_T(J)$  in hand, one may now proceed to compute  $\langle W_f(J) \rangle_x$  and  $\langle W_f(J) \rangle_{I-III}$ .

The expression for  $W_f(J)$  involves a large number of parameters. These include the fission barrier

TABLE IV. Semiempirical fission barriers of Myers and Swiatecki (Ref. 52). Ground-state mass taken from tabulated values of G. T. Garvey, W. J. Gerace, R. L. Jaffe, I. Talmi, and I. Kelson, *Rev. Mod. Phys.* **41**, 51 (1969).

Nucleus	Barrier (MeV)
$^{170}\text{Yb}$	30.6
$^{169}\text{Yb}$	30.5
$^{168}\text{Yb}$	29.5
$^{167}\text{Yb}$	29.0

$B_f$ , the moment of inertia for the saddle shape and the compound nucleus, the pairing corrections to the excitation energy for the compound and the saddle configuration, the value of  $\hbar\omega$ , and the level density parameter  $a$  for the saddle point and the compound nucleus. There are, in principle, values for these parameters which correspond to each residual nucleus in the decay chain of the original  $^{170}\text{Yb}$  compound nucleus. As one could no doubt fit almost any data by freely varying the values of this large number of parameters, we chose to fix the values of all but two of the parameters to those that have been fairly well established in the literature. The only parameters that were varied in order to bring calculated values to within the uncertainties in the experimental data, were the saddle-point level-density parameter and the compound-nucleus level-density parameter. The values of these and the other parameters mentioned above are now discussed.

The fission barriers used in the calculation of  $\Gamma_f$  are the semiempirical barriers of Myers and Swiatecki.<sup>51, 52</sup> The barriers are calculated from experimental ground-state masses and saddle-point masses obtained from a semiempirical mass equation which includes corrections for shell and pairing effects. The fission barriers for the nuclei of concern in the study are given in Table IV.

The saddle-point moments of inertia are taken from the work of Cohen and Swiatecki.<sup>53</sup> Spherical rigid-body moments of inertia are used for the compound nuclei.

As first proposed by Hurwitz and Bethe,<sup>54</sup> odd-even effects are taken into account in the level density calculations by correcting the nuclear excitation energy  $E$  to give an effective excitation energy  $E'$ . This effective energy is given by

$$E' = E \quad \text{for odd-odd nuclei,}$$

$$E' = E - \Delta(n \text{ or } p) \quad \text{for odd } A \text{ nuclei,}$$

$$E' = E - \Delta_p - \Delta_n \quad \text{for even-even nuclei.}$$

The values of  $\Delta_p$  and  $\Delta_n$  calculated by Gilbert and Cameron are used.<sup>55</sup>

The value of 1 MeV is chosen for  $\hbar\omega$  in the fission width calculations.<sup>7</sup> The calculations were found to be insensitive to reasonable variations of this parameter.

The level-density parameter  $a$  appears in the level-density expression for both the fission width and the particle widths. It was found, however, that the calculated fission widths depend primarily upon the ratio of the level-density parameter for the saddle-point configuration and for the compound nucleus  $a_s/a_{cn}$  rather than on their absolute values. Thus, this ratio was ultimately taken as the only free parameter in the calculation.

#### D. Comparison between the theoretically and experimentally determined fissionability

The value of  $a_s/a_{cn}$  is found to be 1.22 when it is required that the calculated value of  $\langle W_f(J) \rangle_{11\text{B}}$  reproduces the experimentally determined value of 0.006. For  $a_s = A/8$ , this implies a value of  $a_{cn} = A/9.8$  which is in reasonable agreement with the usual value of about  $A/10$ . The fission probabilities that result from this ratio of level-density parameters are presented in the last column of Table III and illustrated in Fig. 8. From Table III it may be seen that agreement between experiment and theory is within the experimental error except for the  $^{20}\text{Ne}$  entrance channel where there appears to be a large discrepancy. The discrepancy would disappear if  $J_{\text{CRIT}}$  for the  $^{20}\text{Ne}$  entrance channel were reduced to 63. This lower

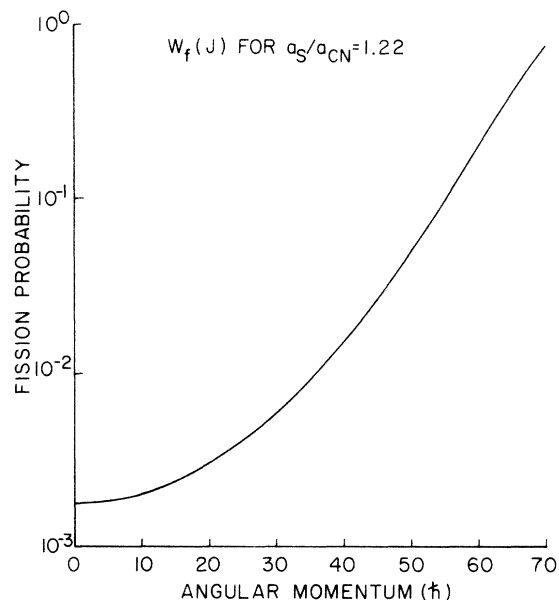


FIG. 8. Graph of  $W_f(J)$  versus  $J$  for  $a_s = A/8$  and  $a_{cn} = A/9.8$  including fissions all along the evaporation chain.

value of  $J_{\text{CRIT}}$  is slightly outside of the uncertainty quoted on the original value of  $J_{\text{CRIT}}$  which arose from the uncertainty in the measured complete-fusion cross section for  $^{20}\text{Ne}$  and implies a value of about 1200 mb rather than 1450 mb.

With the form of  $W_r(J)$  determined, one may proceed to calculate the fission-fragment angular distributions and then compare these predictions to the experimental data.

#### E. Fission-fragment angular distributions

As discussed in Refs. 56 and 57, the fission-fragment angular distribution,  $P_x(\theta)$ , for a particular entrance channel  $x$  may be written as

$$P_x(\theta) \propto \sum_n b_{n,x} P_{n,x}(\theta), \quad (26)$$

where  $b_{n,x}$  is the fractional contribution of the  $n$ th-chance fission to the total fission probability. The quantity  $P_{n,x}(\theta)$  is given by the expression

$$P_{n,x}(\theta) \propto \sum_J (2J+1)^2 T_J^2(x) W_n(J) \times \frac{\exp(-F) I_0(iF)}{\text{erf}[(J+\frac{1}{2})/(2K_0^2)^{1/2}]}, \quad (27)$$

where  $W_n(J)$  is the probability for  $n$ th-chance fission for a compound nucleus with spin  $J$ ,  $I_0$  is the zeroth-order Bessel function,  $K_0^2$  is the variance of the distribution of  $K$  states in the transition-state nucleus, and the quantity  $F$  is given by the expression

$$F \equiv (J+\frac{1}{2})^2 \sin^2\theta / 4K_0^2. \quad (28)$$

It is to be noted that Eq. (27) differs from those previously used in that the angular-momentum dependence of the fission probability  $W_n(J)$  is explicitly introduced.

Values of  $P_x(\theta)$  were calculated according to Eq. (26) for the  $^{11}\text{B}$ ,  $^{12}\text{C}$ ,  $^{16}\text{O}$ , and  $^{20}\text{Ne}$  entrance channels. The calculation was carried out with transmission coefficients both from the sharp-cutoff approximation and with the alternate model described previously with  $J_{\text{CRIT}} - J'$  equal to 10. In Fig. 1 it may be seen that the angular distribution obtained under the sharp-cutoff approximation agrees quite well with that found experimentally. Even somewhat better agreement is found with the alternate model, but the errors due to the uncertainties in the values of  $J_{\text{CRIT}}$  for the various entrance channels do not really allow a firm conclusion on this point. Furthermore, the perturbing effect on the fragment angular distribu-

tions of particle emission from the primary fission fragments was not taken into account in this calculation.

#### V. SUMMARY AND CONCLUSIONS

The experimental data, quite apart from any parameter-dependent theory, clearly illustrate that fissionability is an increasing function of angular momentum for the  $^{170}\text{Yb}$  compound nucleus with 107 MeV of excitation energy. The fact that the excitation energies were matched in the four entrance channels studies avoided masking the angular-momentum dependence by the energy dependence of the fissionability and allowed the determination of the fission probability of compound nuclei with a relatively narrow spread in angular momenta.

The theoretical calculations of fission probability have reproduced the qualitative and quantitative experimental results with a reasonable set of parameters. This substantiates the liquid-drop fission barriers of Myers and Swiatecki as well as the utility of the liquid-drop model in explaining at least the features of the fission phenomenon explored in this work. Within the framework of the parameters used, the saddle-point level-density parameter is greater than the compound nucleus level-density parameter by a factor of about 1.2.

A quantitative comparison between calculated and measured fission cross section implies that the measured  $^{20}\text{Ne}$  complete-fusion cross section is about 350 mb too large, a value which is in excess of the quoted experimental errors by about 100 mb.

The fission-fragment angular distributions have been well accounted for by conventional theory with the addition of the angular-momentum dependence of the fission probability. The relaxing of the sharp-cutoff approximation appeared to result in slightly better agreement, but the degree of improvement is well within the uncertainties involved in the calculations.

#### ACKNOWLEDGMENTS

We wish to thank the operating crew at the Yale heavy-ion accelerator without whose ever-cheerful cooperation this work could not have been carried out. It is a pleasure to record our gratitude for stimulating and useful discussions with Professor M. Blann, Dr. F. Plasil, and Dr. W. Swiatecki.

One of us (JMM) wishes to express his gratitude to the John Simon Guggenheim Memorial Foundation for their support and encouragement.

- \*Work supported by the U. S. Atomic Energy Commission.
- †Present address: Nuclear Chemistry Department, Lawrence Berkeley Laboratory, Berkeley, California 94720.
- ‡Present address: Department of Physics, Montclair State College, Montclair, New Jersey.
- §Present address: Department of Nuclear Medicine, Columbia Presbyterian Hospital, New York, New York 10032.
- ¶Present address: Weizmann Institute of Science, Rehovoth, Israel.
- ||Present address: Department of Chemistry, Marymount Manhattan College, New York, New York 10021.
- \*\*Present address: Department of Chemistry, Florida State University, Tallahassee, Florida 32306.
- <sup>1</sup>N. Bohr and J. A. Wheeler, *Phys. Rev.* **56**, 426 (1939).
- <sup>2</sup>V. M. Strutinski, N. Ya Lyashchenko, and N. A. Popov, *Zh. Eksp. i Teor. Fiz.* **43**, 584 (1962) [transl.: *Sov. Phys.—JETP* **16**, 618 (1963)].
- <sup>3</sup>S. Cohen and W. J. Swiatecki, *Ann. Phys. (N. Y.)* **22**, 406 (1963).
- <sup>4</sup>W. Myers and W. J. Swiatecki, *Nucl. Phys.* **81**, 1 (1966).
- <sup>5</sup>E. K. Hyde, I. Perlman, and G. T. Seaborg, *The Nuclear Properties of the Heaviest Elements III, Fission Phenomena* (Prentice-Hall, Englewood Cliffs, N. J., 1964).
- <sup>6</sup>J. R. Huizenga and R. Vandenbosch, in *Nuclear Reactions*, edited by P. M. Endt and P. B. Smith (North-Holland, Amsterdam, The Netherlands, 1962), Vol. II.
- <sup>7</sup>D. S. Burnett, R. C. Gatti, F. Plasil, P. B. Price, W. J. Swiatecki, and S. G. Thompson, *Phys. Rev.* **134**, 952 (1964).
- <sup>8</sup>S. M. Polikanov and V. A. Druin, *Zh. Eksp. i Teor. Fiz.* **36**, 744 (1959) [transl.: *Sov. Phys.—JETP* **9**, 522 (1959)].
- <sup>9</sup>F. Goldberg, H. L. Reynolds, and D. D. Kerlee, in *Proceedings of the Second Conference on Reactions Between Complex Nuclei* (Wiley, New York, 1960).
- <sup>10</sup>G. E. Gordon, A. E. Larsh, T. Sikkeland, and G. T. Seaborg, *Phys. Rev.* **120**, 1341 (1960).
- <sup>11</sup>H. C. Britt and A. R. Quinton, *Phys. Rev.* **120**, 1768 (1960).
- <sup>12</sup>V. E. Viola, Jr., and T. Sikkeland, *Phys. Rev.* **128**, 767 (1960).
- <sup>13</sup>J. Gilmore, S. G. Thompson, and I. Perlman, *Phys. Rev.* **128**, 2276 (1962).
- <sup>14</sup>F. Plasil, Ph.D. thesis, University of California Radiation Laboratory, 1963 (unpublished).
- <sup>15</sup>V. E. Viola, Jr., T. D. Thomas, and G. Seaborg, *Phys. Rev.* **129**, 2710 (1963).
- <sup>16</sup>T. Sikkeland, *Phys. Rev.* **165**, B669 (1964).
- <sup>17</sup>L. Kowalski, A. M. Zebelman, J. M. Miller, G. F. Herzog, and R. C. Reedy, *Phys. Rev. C* **1**, 259 (1969).
- <sup>18</sup>T. Sikkeland, J. E. Clarkson, N. H. Steiger-Shafui, and V. E. Viola, *Phys. Rev. C* **3**, 329 (1971).
- <sup>19</sup>L. Kowalski, A. M. Zebelman, A. Kandil, and J. M. Miller, *Phys. Rev. C* **3**, 1370 (1971).
- <sup>20</sup>G. A. Pik-Pichak, *Zh. Eksp. i Teor. Fiz.* **34**, 341 (1958) [transl.: *Sov. Phys.—JETP* **7**, 238 (1958)].
- <sup>21</sup>G. A. Pik-Pichak, *Zh. Eksp. i Teor. Fiz.* **43**, 1701 (1962) [transl.: *Sov. Phys.—JETP* **16**, 1201 (1963)].
- <sup>22</sup>J. Hiskes, University of California Radiation Laboratory Report No. UCRL-9275, 1960 (unpublished).
- <sup>23</sup>F. Plasil, private communication.
- <sup>24</sup>E. Gadioli, I. Iori, N. Mohlo, and L. Zetta, *Nucl. Phys.*, *AISI*, **16** (1970).
- <sup>25</sup>R. C. Reedy, M. J. Fluss, G. F. Herzog, L. Kowalski, and J. M. Miller, *Phys. Rev.* **188**, 1771 (1969).
- <sup>26</sup>G. Friedlander, J. W. Kennedy, and J. M. Miller, *Nuclear and Radio Chemistry* (Wiley, New York, 1966).
- <sup>27</sup>Obtained from A. D. MacKay, Inc., 198 Broadway, New York, N. Y.
- <sup>28</sup>Carbon foils obtained from Yissum Research Development Co.; Hebrew University, Jerusalem, Israel.
- <sup>29</sup>Mica obtained from Blanchard Mica Inc., 2315 Broadway, New York, N. Y.
- <sup>30</sup>L. Kowalski, J. C. Jodogne, and J. M. Miller, *Phys. Rev.* **169**, 894 (1968).
- <sup>31</sup>J. B. Natowitz, *Phys. Rev. C* **1**, 623 (1970).
- <sup>32</sup>T. Sikkeland, A. E. Lanski, and G. E. Gordon, *Phys. Rev.* **123**, 2112 (1961).
- <sup>33</sup>V. E. Viola, Jr., and T. Sikkeland, *Phys. Rev.* **130**, 2044 (1963).
- <sup>34</sup>R. Kozub, D. Logan, J. Miller, and A. Zebelman, following paper, *Phys. Rev. C* **10**, 214 (1974).
- <sup>35</sup>P. M. Strudler, I. L. Preiss, and R. Wolfgang, *Phys. Rev.* **154**, 1126 (1967).
- <sup>36</sup>R. M. Diamond, A. M. Poskanzer, F. S. Stephens, W. J. Swiatecki, and D. Ward, *Phys. Rev. Lett.* **20**, 802 (1968).
- <sup>37</sup>V. V. Volkov, G. F. Gridnev, G. N. Zorin, and L. P. Chelmokov, *Nucl. Phys.* **A126**, 1 (1969).
- <sup>38</sup>G. F. Herzog, Ph.D. thesis, Columbia University, 1969 (unpublished).
- <sup>39</sup>G. Galin, B. Gatty, M. Lefort, J. Peter, and X. Tarrago, *Phys. Rev.* **182**, 1267 (1969).
- <sup>40</sup>P. Croft, J. Alexander, and K. Street, *Phys. Rev.* **165**, 1380 (1967).
- <sup>41</sup>R. Kaufman and R. Wolfgang, *Phys. Rev.* **121**, 192, 206 (1961).
- <sup>42</sup>Y. Eyal, K. Beg, D. Logan, J. Miller, and A. Zebelman, *Phys. Rev. C* **8**, 1109 (1973).
- <sup>43</sup>R. C. Reedy, M. J. Fluss, G. F. Herzog, L. Kowalski, and J. M. Miller, *Phys. Rev.* **188**, 1771 (1969).
- <sup>44</sup>R. C. Reedy, Ph.D. thesis, Columbia University, 1969 (unpublished).
- <sup>45</sup>L. Kowalski, A. M. Zebelman, J. M. Miller, G. F. Herzog, and R. C. Reedy, *Phys. Rev. C* **1**, 259 (1970).
- <sup>46</sup>ABACUS-2, E. H. Auerbach, Brookhaven National Laboratory Report No. 6562, 1962 (unpublished).
- <sup>47</sup>E. H. Auerbach and C. E. Porter, in *Proceedings of the Third Conference on Reactions Between Complex Nuclei, Asilomar, 1963*, edited by A. Chiorso, R. M. Diamond, and H. E. Conzett (Univ. of California Press, Berkeley, 1963).
- <sup>48</sup>R. Kaufman and R. Wolfgang, *Phys. Rev.* **121**, 192, 206 (1961).
- <sup>49</sup>R. C. Reedy, Columbia University Report No. CU-1019-72, 1969 (unpublished).
- <sup>50</sup>D. L. Hill and J. A. Wheeler, *Phys. Rev.* **89**, 1102 (1953).
- <sup>51</sup>W. J. Swiatecki, in *Proceedings of the International Conference on Nuclidic Masses, Vienna, Austria, 1963* (Springer-Verlag, Berlin, 1964), Vol. II, p. 58.
- <sup>52</sup>W. D. Myers and W. J. Swiatecki, *Nucl. Phys.* **81**, 1C (1966).
- <sup>53</sup>S. Cohen and W. J. Swiatecki, *Ann. Phys. (N. Y.)* **22**, 406 (1963).

<sup>54</sup>H. Hurwitz and H. Bethe, *Phys. Rev.* 131, 1251 (1953).

<sup>55</sup>A. Gilbert and A. G. W. Cameron, *Can. J. Phys.* 43,  
1446 (1965).

<sup>56</sup>J. M. Gindler and J. R. Huizenga, in *Nuclear Chemis-*

*try*, edited by L. Yaffe (Academic, New York, 1970).

<sup>57</sup>J. R. Huizenga, A. N. Behkami, and L. G. Moretto,  
*Phys. Rev.* 177, 1826 (1969).